# Multiple traps created with an inclined dual-fiber system

**Yuxiang Liu, Miao Yu\***

*Department of Mechanical Engineering, University of Maryland, College Park, MD 20742, USA*
*\*mmyu@umd.edu*

**Abstract:** Multiple optical traps allow one to manipulate multiple particles simultaneously, to characterize interactions in colloidal systems, and to assemble particles into complex structures. Most of the current multiple optical traps are realized with microscope objective-based optical tweezers, which are bulky in size. In this article, we created multiple optical traps with an inclined dual-fiber optical tweezers setup. One 3D trap and two 2D traps were formed at different vertical levels with adjustable separations and positions. We demonstrated that this fiber-based trapping system can be used as a simple block to perform multiple functions, such as particle grouping, separation, and stacking. Moreover, we found that multiple beads can be trapped and stacked up in three dimensions. Compared with those formed with objective-based optical tweezers, the multiple traps presented here are small in size and independent of the objective or the substrate, and hence hold the promise to be integrated in microfluidic systems. This fiber-based multiple traps can be used for on-chip parallel manipulation, particle separation, and characterization of interactions of colloidal and biological systems.

©2009 Optical Society of America

**OCIS codes:** (350.4855) Optical tweezers or optical manipulation; (060.2310) Fiber optics.

---

**References and links**

1. A. Ashkin, "History of optical trapping and manipulation of small-neutral particle, atoms, and molecules," IEEE J. Sel. Top. Quantum Electron. **6**(6), 841–856 (2000).
2. K. C. Neuman, and S. M. Block, "Optical trapping," Rev. Sci. Instrum. **75**(9), 2787–2809 (2004).
3. J. M. Tam, I. Biran, and D. R. Walt, "An imaging fiber-based optical tweezer array for microparticle array assembly," Appl. Phys. Lett. **84**(21), 4289 (2004).
4. J. C. Crocker, and D. G. Grier, "Microscopic measurement of the pair interaction potential of charge-stabilized colloid," Phys. Rev. Lett. **73**(2), 352–355 (1994).
5. Y. Roichman, and D. G. Grier, "Holographic assembly of quasicrystalline photonic heterostructures," Opt. Express **13**(14), 5434–5439 (2005), http://www.opticsinfobase.org/oe/abstract.cfm?URI=oe-13-14-5434.
6. K. Visscher, G. J. Brakenhoff, and J. J. Krol, "Micromanipulation by "multiple" optical traps created by a single fast scanning trap integrated with the bilateral confocal scanning laser microscope," Cytometry **14**(2), 105–114 (1993).
7. G. Boer, R. Johann, J. Rohner, F. Merenda, G. Delacrétaz, Ph. Renaud, and R.-P. Salathé, "Combining multiple optical trapping with microflow manipulation for the rapid bioanalytics on microparticles in a chip," Rev. Sci. Instrum. **78**(11), 116101 (2007).
8. W. Grange, S. Husale, H. Guntherodt, and M. Hegner, "Optical tweezers system measuring the change in light momentum flux," Rev. Sci. Instrum. **73**(6), 2308 (2002).
9. M. P. MacDonald, L. Paterson, W. Sibbett, K. Dholakia, and P. E. Bryant, "Trapping and manipulation of low-index particles in a two-dimensional interferometric optical trap," Opt. Lett. **26**(12), 863–865 (2001).
10. K. J. Moh, W. M. Lee, W. C. Cheong, and X.-C. Yuan, "Multiple optical line traps using a single phase-only rectangular ridge," Appl. Phys. B **80**(8), 973–976 (2005).
11. E. R. Dufresne, and D. G. Grier, "Optical tweezer arrays and optical substrates created with diffractive optics," Rev. Sci. Instrum. **69**(5), 1974 (1998).
12. E. R. Dufresne, G. C. Spalding, M. T. Dearing, S. A. Sheets, and D. G. Grier, "Computer-generated holographic optical tweezer arrays," Rev. Sci. Instrum. **72**(3), 1810 (2001).
13. H. Craighead, "Future lab-on-a-chip technologies for interrogating individual molecules," Nature **442**(7101), 387–393 (2006).

14. F. Merenda, J. Rohner, J. M. Fournier, and R. P. Salathé, "Miniaturized high-NA focusing-mirror multiple optical tweezers," Opt. Express **15**(10), 6075–6086 (2007), http://www.opticsinfobase.org/oe/abstract.cfm?URI=oe-15-10-6075.
15. Y. K. Song, J. Stein, W. R. Patterson, C. W. Bull, K. M. Davitt, M. D. Serruya, J. Zhang, A. V. Nurmikko, and J. P. Donoghue, "A microscale photovoltaic neurostimulator for fiber optic delivery of functional electrical stimulation," J. Neural Eng. **4**(3), 213–218 (2007).
16. D. M. Gherardi, A. E. Carruthers, T. Čižmár, E. M. Wright, and K. Dholakia, "A dual beam photonic crystal fiber trap for microscopic particles," Appl. Phys. Lett. **93**(4), 041110 (2008).
17. K. S. Mohanty, C. Liberale, S. K. Mohanty, and V. Degiorgio, "In depth fiber optic trapping of low-index microscopic objects," Appl. Phys. Lett. **92**(15), 151113 (2008).
18. S. K. Mohanty, K. S. Mohanty, and M. W. Berns, "Organization of microscale objects using a microfabricated optical fiber," Opt. Lett. **33**(18), 2155–2157 (2008).
19. W. Singer, M. Frick, S. Bernet, and M. Ritsch-Marte, "Self-organized array of regularly spaced microbeads in a fiber-optical trap," J. Opt. Soc. Am. B **20**(7), 1568 (2003).
20. K. Taguchi, K. Atsuta, T. Nakata, and M. Ideda, "Levitation of a microscopic object using plural optical fibers," Opt. Commun. **176**(1-3), 43–47 (2000).
21. Y. Liu, and M. Yu, "Investigation of inclined dual-fiber optical tweezers for 3D manipulation and force sensing," Opt. Express **17**(16), 13624–13638 (2009), http://www.opticsinfobase.org/oe/abstract.cfm?URI=oe-17-16-13624.
22. R. C. Gauthier, "Optical trapping: a tool to assist optical machining," Opt. Laser Technol. **29**(7), 389–399 (1997).
23. W. Grange, S. Husale, H. Guntherodt, and M. Hegner, "Optical tweezers system measuring the change in light momentum flux," Rev. Sci. Instrum. **73**(6), 2308 (2002).
24. W. H. Wright, G. J. Sonek, and M. W. Berns, "Parametric study of the forces on microspheres held by optical tweezers," Appl. Opt. **33**(9), 1735 (1994).
25. J. Guck, R. Ananthakrishnan, H. Mahmood, T. J. Moon, C. C. Cunningham, and J. Käs, "The optical stretcher: a novel laser tool to micromanipulate cells," Biophys. J. **81**(2), 767–784 (2001).

## 1. Introduction

Optical tweezers (OTs) have been widely used for non-contact manipulations of micro- or nano-sized particles since they were invented by Ashkin *et al* in 1986 [1]. When the light from OTs is incident on and deflected by the surface of an object, optical forces are applied to the object due to the photon momentum change. With the help of OTs, single molecules have become accessible units to biologists and physicists [2]. Although OTs were originally designed to manipulate a single particle at a time [3], multiple optical traps that can provide simultaneous manipulation of multiple particles are desirable in many applications. Multiple optical traps have been used to characterize the interactions of colloidal systems [4], to assemble particles into complex structures [5], and to trap and orient delicate particles [6]. Various techniques have been employed to generate multiple optical traps, such as one or two objectives with multiple input beams [4,7,8], time-sharing approaches with a scanning laser beam [6], interference of multiple beams [9], fringes created with a phase-only rectangular ridge [10], diffractive optics [11], and, more commonly, computer-generated holograms [5,12]. All of these methods make use of traditional objective-based OTs, which are bulky, expensive, and hard to integrate.

Particle manipulation methods that can provide multiple traps in parallel and be readily integrated in miniaturized systems for biological analysis and diagnostics [7,13], e.g., lab-on-a-chip systems, are of great interest. In these integrated and scaled-down devices, the large objectives needed to enable optical traps have to be replaced by smaller units. In literature, an array of parabolic micromirrors has been used to create multiple traps with each trap formed at the focus of a micromirror [14]. Compared with these embedded micromirrors, optical traps built with optical fibers provide a more flexible solution towards compact, integrable multiple traps. Optical fibers are small in size and biocompatible [15], and therefore can be potentially integrated in a lab-on-a-chip system for biological applications. Multiple two-dimensional (2D) optical traps have been realized previously with a bundle of optical fibers [3], in which each individual fiber forms a separate trap. More recently, counter-propagating dual photonic crystal fiber traps have been demonstrated to confine multiple particles in the intensity minima or maxima of the standing waves [16]. In another work, a Bessel beam emitted from a

single optical fiber with an axicon-shaped fiber tip has been employed to trap multiple particles with a low refractive index [17]. For the abovementioned fiber-based multiple traps built with fiber bundles and standing waves, the separations between the traps cannot be adjusted. In addition to multiple optical traps, optical binding using fiber-based systems has also been exploited to confine particles of micrometers or sub-micrometers, such as the single optical fiber with an axicon-shaped fiber tip [18] and the counter-propagating dual fiber traps [16,19]. The optical binding effects can be explained as that multiple particles are distributed in a self-organized way, due to the interaction between the particles and the optical field, to minimize the energy of the whole particle-light system [19]. The fiber-based optical binding introduced above can only confine particles in a chain-like one-dimensional structure with fixed particle separation.

In this paper, we report multiple optical traps built with an inclined dual-fiber optical tweezers (DFOTs) system. A similar system has been reported to form a single trap for particle levitation [20]. In our previous work, the performance of the 3D trap was investigated both experimentally and numerically [21]. Here, we formed three optical traps on different vertical planes, one 3D trap below the beam intersection and two 2D traps on the cover glass. The inclined DFOTs system can be controlled as a whole block containing two fibers, resulting in controllable positions of the three traps with a single actuator. The trap separations are readily tunable by changing the vertical position of the block. We demonstrate experimentally that the multiple traps can perform multiple functions: particle separation, particle stacking, and particle grouping. We observed in the experiment that multiple beads were trapped in three dimensions. The optical forces on the $yz$ plane are investigated numerically. Particle separation and stacking and 3D trapping of multiple beads are explained according to the force field obtained from the simulation results. Different from the fiber-based multiple traps and optical binding reported in the literature, no additional actuator is needed in order to adjust the separations between the traps, which makes the inclined DFOTs system simpler and more flexible.

## 2. Experiment

### 2.1 Experimental setup

The inclined DFOTs system is built on the platform of an inverted microscope (CKX41, Olympus Inc.), as shown in Fig. 1. Light from an 808 nm fiber-coupled laser diode (FMXL808-080SA0B, Bluesky Research) is equally split into two lensed fibers (OZ Optics). The optical beams exiting from the lensed fibers are used to form optical traps in water. Each lensed fiber is attached to a miniature 3D translation stage (07TMC521, CVI Melles Griot) to facilitate fiber alignment. The fibers are aligned before experiment once and for all. Both stages are fixed on a board so that they can be moved together as a block by a third 3D stage. The fibers are arranged to form an inclination angle $\theta$ of 50° with respect to the vertical axis $z$ (see Fig. 2). The separation between the fiber tips is 45 μm along the $y$ direction. The optical beam emitted from each lensed fiber has a beam waist of 1.35 μm, which is located 12 μm from the fiber endface. The total optical power emitted from both fibers is 21.0 mW. A coverglass with a water drop containing silica beads (Bangs Laboratories, Inc.) is placed on a two-dimensional stage. The silica beads have a diameter of 4.74 μm, a density of 2.0 g/cm$^3$, and a refractive index of 1.45. The experiment is monitored with an oil-immersion objective (PlanC N 100 × /1.25, Olympus Inc.) and recorded with a CCD camera (Moticam 1000, Motic).

### 2.2 Trapping principle of the multiple traps

In the inclined DFOTs shown in Fig. 2, there are one 3D trap formed at Bead 2 and two 2D traps at Bead 1 and 3. For Bead 2, each beam induces a scattering force [1] that is along the light propagation direction and a gradient force [1] that is opposite to the intensity gradient

(i.e., towards the optical axis). Bead 2 is trapped in three dimensions when the four forces applied by the two beams, two transverse gradient forces ($F_{g1}$ and $F_{g2}$) and two scattering forces ($F_{s1}$ and $F_{s2}$), are balanced. The equilibrium position is slightly below the intersection of the two beams [21]. It is noted that the gravity and buoyancy are important to consider whether a 3D trap can be formed, although they are not shown in Fig. 2. The 2D traps at Bead 1 and Bead 3 are similar with each other due to symmetry, so we only discuss the trapping of Bead 1. The beam from Fiber 1 is much further away from Bead 1 than that from Fiber 2, so we only consider the optical forces applied by the beam from Fiber 2. When the gradient force ($F_g$) and the scattering force ($F_s$) reach equilibrium with the normal force ($N$) applied by the substrate, Bead 1 is trapped on the substrate. By moving the two fibers as a block, the separations between the traps as well as the trap positions can be adjusted.
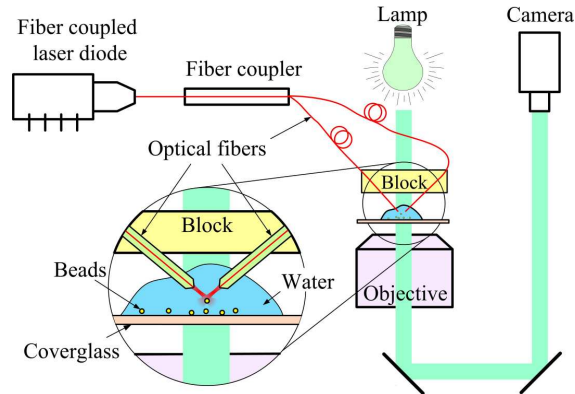


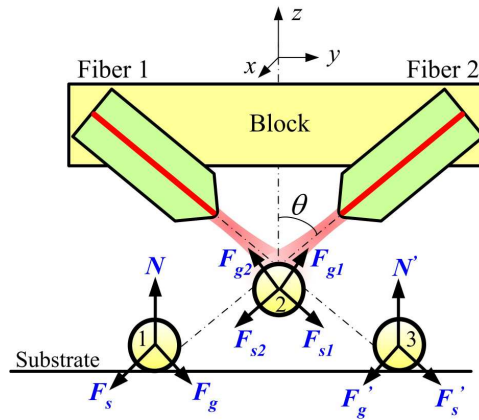Fig. 1. Schematic of the inclined DFOTs system.



Fig. 2. Principle of multiple traps created by using the inclined DFOTs.

*2.3 Demonstration of multiple traps and particle separation*

The images captured consecutively from a video clip of the multiple traps are shown in Fig. 3. There were five beads in the field-of-view, each labeled with a number to track their movement. The two shadows on both sides of the pictures are the fiber tips, which are out-of-focus and blurry. The beam intersection was initially close to the coverglass, which formed an aura as can be seen in the center of Fig. 3(a). With the coverglass moved around, Beads 1, 2, and 3 were trapped, as shown in Fig. 3(b). The three trapped beads were in contact with each other due to the position of the beam intersection. Beads 4 and 5 were free reference beads, which were lying on the coverglass and could be moved together with the coverglass. When

the fiber block was moved along $+z$ direction, the three trapped beads were separated: the separation between Beads 1 and 3 increased and Bead 2 was lifted up from the coverglass, as shown in Figs. 3(b)–3(d). At this moment, Bead 2 was trapped in three dimensions while Beads 1 and 3 were trapped in two dimensions on the coverglass. Then, the traps were fixed and the coverglass was moved in $xy$ plane (see Fig. 3(d)–3(f)). During this process, all three traps remained stable. As the height of the fiber block was increased further, the two 2D traps became weaker and weaker. Beads 1 and 3 were found to remain trapped when the height of Bead 2 was up to 30 μm above the coverglass (the separation between Beads 1 and 3 were around 70 μm).
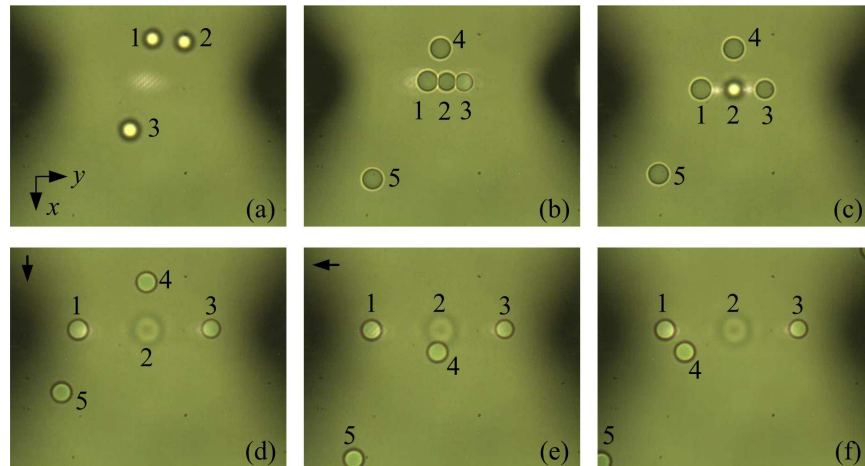


Fig. 3. Images of beads manipulated using the multiple traps. (a) Three free beads were lying on the coverglass. (b) Beads 1, 2, and 3 were trapped in contact. (b)-(d) The fiber block was moved upward along $+z$ and trapped beads were separated. (d)-(f) The coverglass was moved along $+x$ and then along $-y$. The arrows in (d) and (e) indicate the next movement direction of the coverglass. The $xy$ coordinate system is shown at the lower left corner of (a). The bead size is 4.74 μm in diameter.

These experimental results demonstrate that the inclined DFOTs can be used to simultaneously manipulate multiple particles at different vertical levels as well as align particles in line. The positions and separations of the three traps can be controlled by moving the fiber block. When the fiber block is lifted up, both the height of the 3D trap and the separation between the two 2D traps are increased, rendering the ability to separate particles that stick together. In addition to particle separations, the multiple traps created with the inclined DFOTs also bestow this setup the capability of particle stacking, particle grouping, and trapping multiple particles in three dimensions, which will be detailed next.

*2.4 Particle stacking*

To better demonstrate particle stacking, four beads were trapped initially by the multiple traps, as shown in Fig. 4(a). At this moment, Bead 2 was trapped in the 3D trap, and the rest of the beads were trapped by the two 2D traps, as illustrated in Fig. 4(d). When the beam intersection was brought close to the coverglass by lowering down the fiber block, the separations between the four beads became smaller, as shown in Fig. 4(b) and Fig. 4(e). As the fiber block was lowered down further, Beads 1, 2, and 3 became in contact with each other, and Bead 4 was stacked up above Bead 3, as shown in Fig. 4(c) and Fig. 4(f).
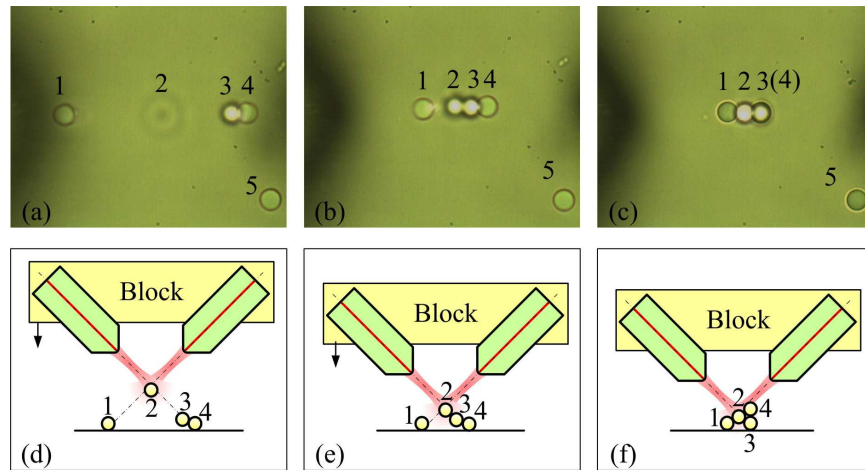
Fig. 4. Experimental demonstration of particle stacking. With the fiber block lowered down toward the coverglass, the four beads were (a) first separated, (b) then brought into contact, and (c) finally stacked. (a)-(c): pictures captured from a video clip; (d)-(f): sketches illustrating pictures (a)-(c), respectively. The bead size is 4.74 μm in diameter.
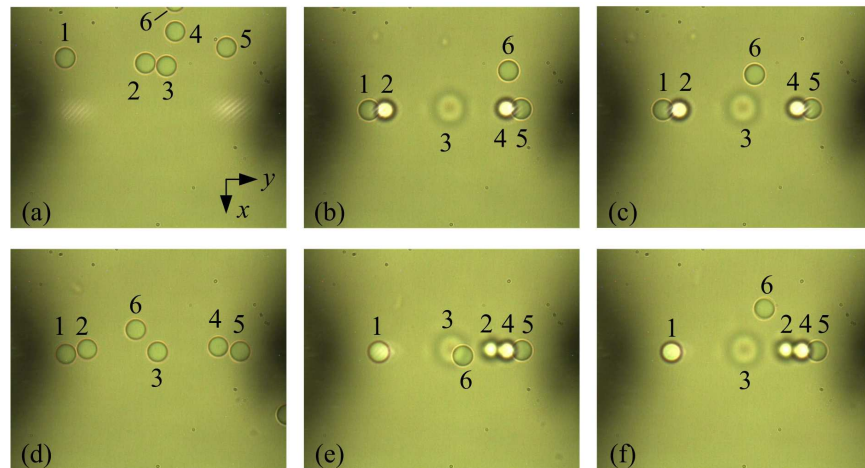


Fig. 5. Experimental demonstration of particle grouping. (a) Six free beads were initially lying on the substrate. (b) Beads 1 to 5 were trapped and separated into three groups. Bead 6 was free and served as the reference of the coverglass movement. (c) The coverglass was move along -y. (d) The laser was switched off and all beads return to the coverglass. (e) After the laser was turned on, Beads 1 to 5 were separated into three new groups, while Bead 6 remained free. (f) The coverglass was moved along –x. The bead size is 4.74 μm in diameter.

## 2.5 Particle grouping

For particle grouping, five beads (Beads 1 to 5) were first separated into three groups by the three traps created by the inclined DFOTs, as shown in Fig. 5(b). Each 2D trap confined two beads in a group and the 3D trap trapped one bead above the other two groups. As the coverglass was moved along -y direction (Fig. 5(c)), Beads 1 to 5 remain trapped in the three groups. The laser was then switched off to allow all beads freely return to the coverglass and regroup. After regrouping, one bead (Bead 1) was trapped solely by one of the 2D traps, and three other beads (Beads 2, 4 and 5) were trapped in a group by the other 2D trap, with another bead (Bead 3) trapped by the 3D trap, as shown in Fig. 5(e). When the coverglass was moved in -x direction (Fig. 5(f)), the five beads remained trapped in their groups, indicating that the traps and grouping were stable. It should be noted that there is an upper limit of the

number of particles that can be grouped. The number of particles that can be trapped in each trap is limited by both the beam parameters (e.g., power, size, and wavelength) and the particle size. With the beam parameters and the particle size used in our experiment, the largest number of trapped particles in one 2D trap is three. The largest number of particles that can be trapped by the 3D is also three, which will be shown in Section 2.6. This implies that the largest number of particles that can be grouped is nine.
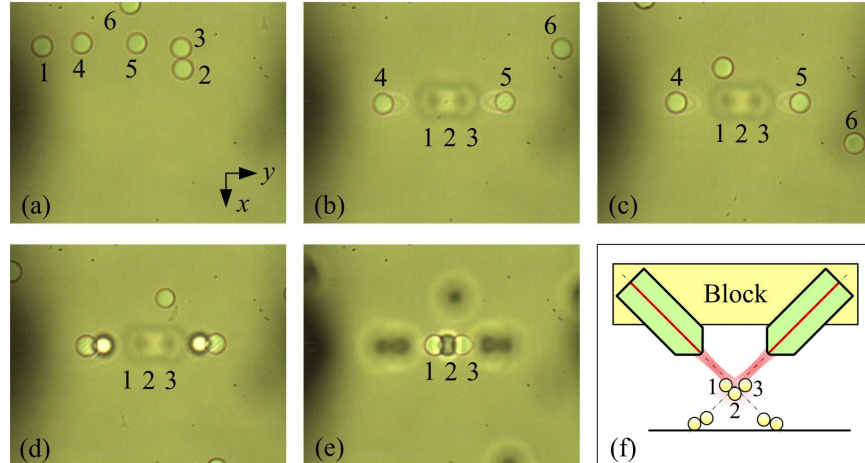


Fig. 6. Experimental demonstration of multiple particles trapped in three dimensions. (a) Six free beads were lying on the coverglass. (b) Beads 1, 2, and 3 were trapped by the 3D trap, and Bead 4 and 5 were trapped by the 2D traps. Bead 6 was free and served as the reference of the coverglass movement. (c) The coverglass is moved along + $x$, with the trapped beads staying stable. (d)–(e) The objective lens was moved along + $z$ direction. Bead 2 was first brought into focus before Beads 1 and 3 (see the media). Beads 1 and 3 were in focus in (e). (f) The sketch illustrating the images (d) and (e).

## *2.6 Trapping multiple particles in three dimensions*

In addition to 3D trapping of single particles reported previously [20,21], the 3D trap of the inclined DFOTs system was found to be able to trap multiple traps in three dimensions. Six free beads stayed rest on the coverglass initially as shown in Fig. 6(a). When the fiber block was lowered down and then lifted up, three beads (Beads 1, 2, and 3) were trapped by the 3D trap, as shown in Fig. 6(b). As the coverglass was moved in the $x$ directions, the trapping of the three beads remained stable, as shown in Fig. 6(c). Each of the 2D traps was still able to trap two beads with three beads trapped by the 3D trap, as shown in Fig. 6(d). As the objective was moved upwards along the z direction, Bead 2 was brought into focus before Beads 1 and 3, which implies that Beads 1 and 3 were located higher along the z direction than Bead 2. Figure 6(e) shows that Bead 2 was out of focus when Beads 1 and 3 were in focus.

The experiments discussed above demonstrate that the inclined DFOTs have the ability of creating multiple optical traps. With two fibers assembled on a block, control of the positions as well as the separations of the traps can be realized easily. With a single actuator, in our case, a 3D translation stage, attached to the fiber block, particle separation, stacking, and grouping can be achieved.

## 3. Simulations

Based on a ray-optics model [21,22], numerical simulations have been carried out to better understand the experimental results. The parameters used to obtain the simulation results are consistent with those used in the experiment to be the same as those used in the experiments.

The net force ($F_n$) of the optical force, gravity, and buoyancy experienced by a bead in the trapping area is mapped on the $yz$ plane, as shown in Fig. 7(a). Each arrow represents the net force applied on a bead that is centered at the starting point of the arrow. The arrow direction and length indicate the force direction and magnitude, respectively. The optical axes (dash-dotted lines) of the two optical beams exiting from the two fibers are plotted in Fig. 7(a), which intersect at the origin of the $xyz$ coordinate system. It should be noted that here, the optical forces are obtained under the assumption that only one bead exists in the optical field. However, in the real experimental situation that multiple beads are trapped, the distortion of the optical field by the upstream beads will influence the optical force applied on the downstream beads. This influence is beneficial to the trapping of downstream beads, because the upstream beads focus the light as a lens and the intensity gradient of the light can be increased, resulting in tighter downstream traps.
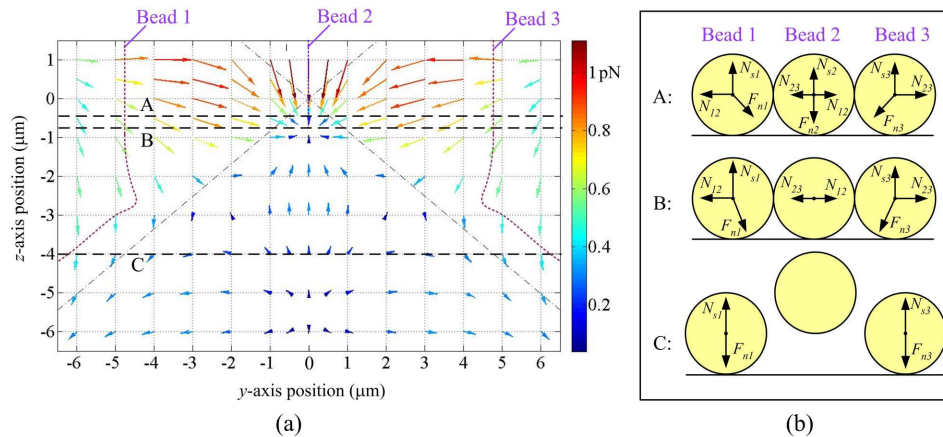


Fig. 7. (a) The $yz$ plane force field of $F_n$ (the net force of the optical force, gravity, and buoyancy, excluding the normal forces between the beads and between the beads and the coverglass); (b) free body diagrams of three beads (Beads 1, 2, and 3) at three different vertical levels shown in (a): Level A, B, and C. $F_{ni}$ stands for $F_n$ of Bead i. $N_{si}$ and $N_{ij}$ stand for the normal forces between the substrate (the coverglass) and Bead i and between Beads i and j, respectively.

Bead separation observed in the experiment can be explained according to the simulation results. Three beads corresponding to Beads 1, 2, and 3 in Fig. 3 are considered lying on a coverglass and located near the beam intersection initially. When the coverglass is moved along $-z$ direction, the trajectories of the three trap positions (dotted curves in Fig. 7(a)) are obtained as the equilibrium positions of the bead centers corresponding to different vertical levels of the coverglass. The equilibrium of Bead 2 is always located on the $z$ axis due to symmetry of the system. The free body diagrams of the trapped beads centered at three different vertical levels A, B, and C are shown in Fig. 7(b). According to the simulations (data not shown), the 3D trap is located 0.87 μm below the beam intersection (i.e., at point (0, 0, −0.87 μm)), where the net force ($F_n$) is zero. It is noted that this 3D trap position is the lowest equilibrium position of Bead 2. When the three beads are located above the 3D trap, for example, at $z = -0.5$ μm (Level A in Fig. 7(a)), i.e., the coverglass is 2.87 μm below the beam intersection, the $y$-components of $F_{n1}$ and $F_{n3}$ are pointing to the center bead (Bead 2). Therefore, the normal forces ($N_{12}$ and $N_{23}$) are formed between the three beads. At the same time, the coverglass prevents the beads from being pushed down by the $z$-components of $F_{n1}$ and $F_{n3}$. This corresponds to the experimental results shown in Fig. 3(b). As the coverglass is moved along $-z$ direction, the net force ($F_{n2}$) applied to Bead 2 decreases and the normal forces ($N_{12}$ and $N_{23}$) become smaller. At $z = -1.03$ μm (Level B), $F_{n2}$ reaches zero and the

normal force ($N_{s2}$) disappears, while Beads 1 and 3 are still pushed against the coverglass by $F_{n1}$ and $F_{n3}$. As the coverglass is lowered beyond Level B, Bead 2 is lifted up from the coverglass and Beads 1 and 3 are pushed towards each other by $F_{n1}$ and $F_{n3}$, respectively. This explains the reason why the trajectories of Beads 1 and 3 curve slightly inside towards the $z$ axis. In experiment, this effect was observed as bead stacking, as shown in Fig. 4. As the coverglass is lowered further, the $y$-components of $F_{n1}$ and $F_{n3}$ gradually change their directions and point away from the $z$ axis, which results in the separation of Beads 1 and 3. For example, at $z = -4$ μm (Level C), Beads 1 and 3 separate and eventually settle at the positions of $y = -6.2$ μm and 6.2 μm, respectively. These simulation results can be used to explain the experimental results shown in Figs. 3(c)-3(f). It is noted that the above discussions are based on the condition that the beads fall down from a position above the beam intersection. If, in another case, the beads are originally located below the beam intersection with Bead 2 centered on the z axis, Beads 1 and 3 will still be trapped in the 2D traps, but the trajectory of Bead 2 will depend on its original position [21]. If the net force points up at its original position (for example, $z = -4$), Bead 2 will be lifted and trapped by the 3D trap. Otherwise, Bead 2 will be pushed downwards along the $z$ axis. Due to the Brownian motion, Bead 2 will move away from the $z$ axis randomly (either towards left or right), and eventually it will settle at one of the 2D traps.
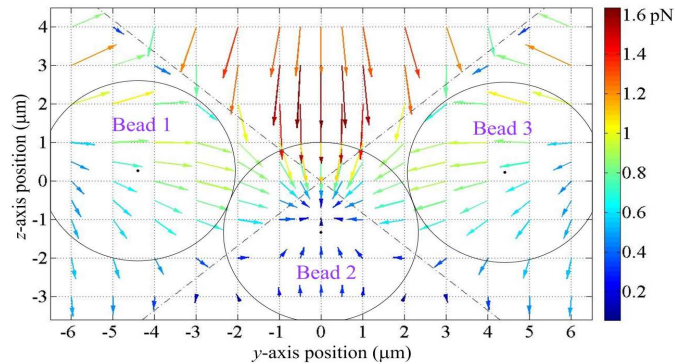


Fig. 8. The $yz$ plane force field of $F_n$ (the net force of the optical force, gravity, and buoyancy, excluding the normal forces between the beads). Beads 1, 2, and 3 are trapped in three dimensions.

Multiple beads 3D trapping can also be explained by the simulation results. Beads 1, 2, and 3 in Fig. 8 correspond to the three 3D trapped beads shown in Fig. 6. Beads 1 and 3 are pushed towards the beam intersection (0, 0) by the optical forces, while the normal forces between the beads prevent Beads 1 and 3 from moving along the $y$ and $z$ axes. Bead 2 is pushed by the normal forces downward (along -$z$) from its original equilibrium (0, 0, −0.87 μm), resulting in an upward optical force applied on Bead 2. Bead 2 reaches new equilibrium when the optical force balances the normal forces applied by Beads 1 and 3. In this case, all three beads are trapped stably in three dimensions.

Bead stacking shown in Fig. 4 can also been explained. When the coverglass is close to the beam intersection, the outer beads (Beads 1, 3, and 4) are pushed inside by the optical forces (data not shown). If there is a small perturbation of the $z$ position of Bead 4 due to Brown motion, Bead 4 will "climb" over Bead 3, which explains the experimental results shown in Fig. 4.

## 4. Discussions

The experiment and the simulations demonstrate that the inclined DFOTs have the ability to create multiple traps. The positions of the traps can be controlled by controlling the position

of the fiber block with a single actuator. The fiber block can also be rotated to change the orientation of the plane on which the three traps are aligned. Moreover, the separations between the three traps can be adjusted by simply tuning the height of the fiber block without bringing in another actuator. As the position of the fiber block is moved higher, both the height of the 3D trap and the separation between the two 2D traps can be increased. However, because the single actuator on the fiber block cannot provide enough degrees of freedom, the three traps cannot be adjusted independently, like what the holographic OTs can achieve [5,12]. The height of the 3D trap is coupled with the separation between the two 2D traps. The ability of the inclined DFOTs for particle stacking implies that they can potentially be used for arranging trapped particles in a 3D pattern. As shown in Fig. 6, seven trapped particles are arranged in four layers along the $z$ direction. Due to the limitation of the current setup, no more than four layers along the $z$ axis can be achieved. However, along the $x$ axis, multiple fiber blocks can be introduced to create multiple layers of the trapped particles. Due to the physical size of the optical fibers (~100 μm), there will be a minimum achievable separation between the adjacent layers. To further reduce the layer separation along the $x$ direction, the optical fibers can be thinned with hydrofluoric acid (HF) etching.

Although the current single inclined DFOTs setup can only create three traps, it is possible to create a large number of traps by integrating multiple inclined DFOTs due to the flexibility and compact size offered by this setup. In addition to the potential to be integrated, the fact that neither the objective nor the substrate plays a role in forming the traps bestows the inclined DFOTs advantages over objective-based OTs. The working distance (the distance that the 3D trap can be moved up) of the inclined DFOTs is not constrained by the substrate whereas that of the traps created with an objective is limited by the working distance of the objective, which is typically within 20 μm from the substrate for an oil immersion objective [23]. If imaging is not considered, the multiple traps created by the inclined DFOTs can work with any substrate, which is desirable for chip-based systems that use silicon or other lightproof substrates. It is worth noting that compared with the objective-based OTs, the trap quality of the inclined DFOTs is less susceptible to the location of the beam waist and the focus strength. This is due to the fact that the axial gradient force that is used to balance the scattering force for the objective based OTs is strongly influenced by the beam waist location and the strength of the focusing effect [24]. By contrast, the inclined DFOTs use the transverse gradient force from the other beam to balance the scattering force, and thus are more robust to the beam waist position and focus strength. In fact, it was found experimentally that when the beam intersection was around 17 μm downstream from the beam waists, the multiple traps were still retained. There is another advantage of the inclined DFOTs compared with objective based OTs, which is a higher allowable optical power. When used for manipulation of biological particles, because the beam spots at the traps are much larger for the inclined DFOTs, they can induce less damage to biological tissues than objective-based OTs at the same power. According to Reference [25], an optical power as high as 800 mW for each beam can be used without optical damage to the trapped cells in the optical stretcher. Due to the fact that the gradient forces need to overcome the scattering forces in order to achieve a 3D trap, the optical forces induced by the inclined DFOTs in the $yz$ plane are smaller than those generated with objective based OTs (on the order of 1 pN per 10 mW [2]). However, one can increase the optical power to achieve a larger trapping force. It should also be noted that the $x$-axis optical forces of the inclined DFOTs, which are ~8 pN per 10 mW from each fiber [21], are at the same level as those of the objective based OTs.

## 5. Conclusions

Multiple optical traps, one 3D and two 2D traps, have been created at different vertical levels with an inclined dual-fiber optical tweezers setup. The positions of the multiple traps are controllable by moving the fibers as a block. The separations of the traps are tunable with a single actuator attached to the block. Particle separation, stacking, and grouping have been

demonstrated with the multiple traps. Multiple beads were trapped in three dimensions and stacked up without contact with the substrate. The optical force field is investigated numerically to explain and understand the experimentally observed multiple functions of the inclined DFOTs. The inclined dual-fiber optical tweezers have potential to be integrated in microfluidic systems for parallel manipulation of micro-sized particles. The ability to separate particles that stick together endows this system the capability to study interactions in colloidal systems. The 3D trapping and stacking of multiple particles indicates that this system can potentially help arrange particles into 3D lattices.